Embedded Liquid Cooling of High-Power Microelectronics Using Liquid Metal

Huicheng Feng
*Institute of Microelectronics, A*STAR*
Singapore
fenghc@ime.a-star.edu.sg

Bin He
*Institute of Microelectronics, A*STAR*
Singapore
heb@ime.a-star.edu.sg

Gongyue Tang
*Institute of Microelectronics, A*STAR*
Singapore
tangg@ime.a-star.edu.sg

Xiaowu Zhang
*Institute of Microelectronics, A*STAR*
Singapore
xiaowu@ime.a-star.edu.sg

Boon Long Lau
*Institute of Microelectronics, A*STAR*
Singapore
laubl@ime.a-star.edu.sg

Keng Yuen Jason Au
*Institute of Microelectronics, A*STAR*
Singapore
auky@ime.a-star.edu.sg

Jun Wei Javier Ong
*Institute of Microelectronics, A*STAR*
Singapore
ongjwj@ime.a-star.edu.sg

Ming Chinq Jong
*Institute of Microelectronics, A*STAR*
Singapore
mcjong@ime.a-star.edu.sg

***Abstract*—Liquid metals have high thermal conductivities and shows great potential in liquid cooling of high-power microelectronics. This paper studies embedded liquid cooling using liquid metal (eutectic GaInSn). A thermal test vehicle (TTV) is fabricated for cooling performance analysis. It is deposited with a heater and two resistance temperature detectors (RTDs) for heating and temperature monitoring, and etched with embedded micro-pin fins for cooling enhancement. The TTV is tested with GaInSn and deionized water. Numerical simulations are conducted using ANSYS Fluent and validated with test data. A temperature discrepancy between tests and simulations in the inlet area is found in GaInSn cooling. It is attributed to the poor wetting in the inlet area (near RTD1) due to the large Laplace pressure of GaInSn in the TTV. The finding suggests that in addition to thermal properties, surface tension also needs to be considered when designing and developing liquid metal micro-coolers. Our simulation results show that GaInSn without fins shows better cooling effect compared to deionized water with fins. Besides, for the case of no fins, GaInSn cooling achieves much lower chip temperature, higher heat transfer coefficient with a slightly lower coefficient of performance compared to deionized water. It means that the geometry of liquid metal micro-cooler can be greatly simplified without compromising the cooling performance. Further experimental studies are be conducted for verification.**

Keywords*—*liquid metal cooling, embedded cooling, high-power microelectronics

I. INTRODUCTION

Following Moore's Law of ICs or Moore's Law of Packaging, with the further development of microelectronics, the thermal design power, and more importantly, the power density of chips continues to increase [1-3]. Therefore, heat dissipation becomes the key to further high-level integration of microelectronics. Advanced and high-efficient cooling technologies are demanded. Researchers proposed and developed various kinds of cooling methods to maximize the cooling capacity, such as jet impingement, micro-channels, micro-pin fins, hierarchical manifold micro-channels, and two-phase liquid cooling [4-11]. Two-phase liquid cooling commonly encounters highly fluctuated chip temperature and system pressure [12-15], which may cause chip failure due to the temporal over-heating. Complex micro- and nano- structures in micro-cooler are commonly fabricated to enhance heat transfer between the chip and the coolant (such as deionized water and Novec-7300) as these conventional coolants have low thermal conductivities. This generally comes with a price of complex fabrication process and high flow resistance.

Liquid metals have much higher thermal conductivities compared to conventional coolants (Table I) and are widely used in the cooling systems of solar energy, nuclear fusion, *etc*. [16-18] They are also attracting attention from researchers in microelectronics [19-20]. Many studies utilizing liquid metals or liquid metal-based composites as thermal interface materials. For example, Lin *et al*. [21] used liquid metal-based composites as thermal interface material in a cell phone and achieved 5.9°C temperature reduction compared to commercial silicon pad. Some studies adopted liquid metals as coolant for heat dissipation and achieved a lower thermal resistance compared to water in power modules [22].

Table I Coolant physical properties at 25°C.

	DI Water	**Novec 7300**	**GaInSn[a]**
Density (kg/m^3)	997	166	6370
Thermal conductivity (W/m.K)	0.6	0.062	24.9
Specific heat capacity (J/kg.K)	4182	1140	390
Dynamic viscosity (mPa.s)	0.89	1.18	5.3
Electrical conductivity (S/m)	5.5×10^{-6}	\	24.9
Surface tension (N/m)	0.072	0.015	0.605

[a.] Eutectic alloy of Ga, In, and Sn (LMTG10B, alloykingdom).

Embedded liquid cooling has low thermal resistance and is a promising cooling method for high-power microelectronics such

This research was supported by the Agency for Science, Technology and Research (A*STAR) under Council Strategic Fund (Grant No. C210415009) for design & modelling, assembly process, manifold design & fabrication, and testing, and Applied Centre of Excellence in Advanced Packaging 3.0 (Grant No. I2101E0008) for wafer process development.

as 3D ICs. In our previous study, we experimentally investigated embedded two-phase liquid cooling of deionized water [23-24]. In this study, we utilize liquid metal, eutectic GaInSn, as coolant and analyzes its cooling performance in an embedded micro-cooler. Experimental tests and analysis reveal that, unlike deionized water, surface tension, in addition to the thermal properties, is an important influencing factor in the design of liquid metal micro-cooler. In addition, the simulation results show that liquid metal achieves a much lower chip temperature and works well without the micro-pin fins. This means that the geometry of liquid metal micro-cooler can be greatly simplified without compromising its cooling performance.

II. METHODS

A thermal test vehicle (TTV) is designed and fabricated (Fig. 1). It consists of a silicon chip, a silicon cap, and a PCB. The silicon chip and cap are of a footprint of 10 mm × 10 mm and a height of 0.3 mm. The silicon chip has a titanium thin film heater and two resistance temperature detectors (RTDs) deposited on the front and micro-pin fins etched on the back. The electrical resistances of heater and RTDs are 440 Ω and 720 Ω, respectively. The staggered micro-pin fins are of diameter 100 µm, pitch 150 µm, and height 220 µm. The silicon cap is bonded to the chip back, forming a micro-cooler with inlet and outlet on the sidewalls. A PCB is designed, fabricated, and bonded to the chip front to power the heater and collect chip temperatures from RTDs. The detailed fabrication process can be referred from [25].

A manifold is designed and fabricated to feed in and collect coolant from the TTV. The manifold is CNC machined with Torlon 5530, and assembled with the TTV using screws (Fig. 2). The experimental setup is built for testing and characterization. A MD scientific syringe pump is used to drive and control the coolant flowrate.

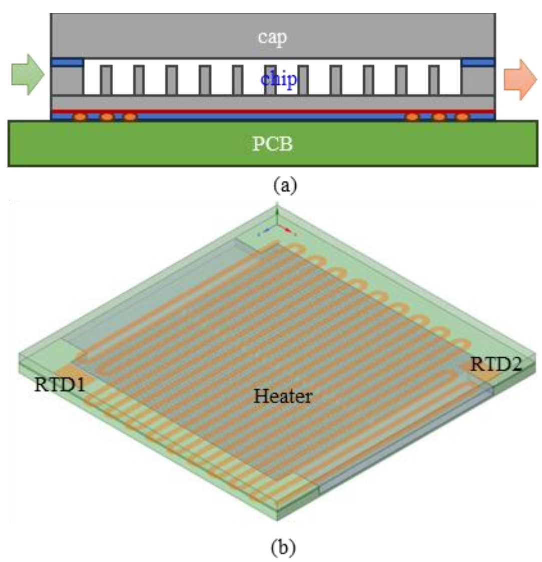

Fig. 1 (a) Cross-sectional and (b) isometric views of TTV.

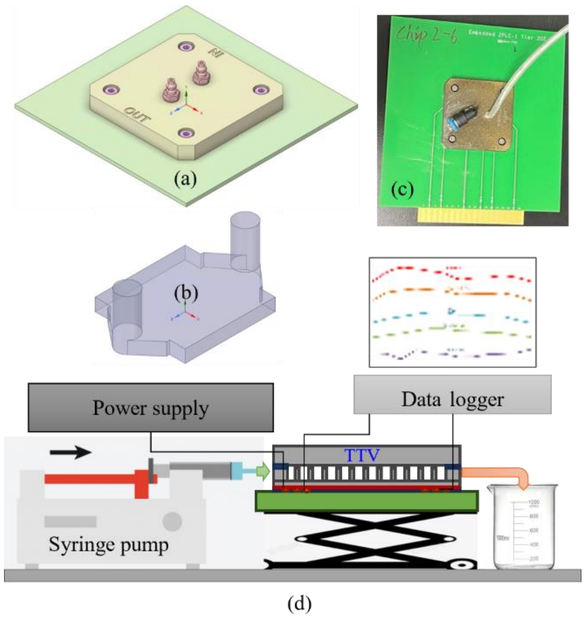

Fig. 2 (a) The manifold, (b) coolant flow inside manifold, (c) TTV assembled with the manifold, and (d) experimental setup.

Numerical simulations are performed using ANSYS software. The geometric model is drawn in SpaceClaim, meshed using Fluent Meshing, and computed with Fluent. Since it is microscale, low fluid velocity, the energy equation is solved in laminar flow regime. We refined the meshes until the simulation results show negligible variations with further refinement (<1%). The residuals of continuity and momentum equations are set as 10^{-6}, and that of energy equation set as 10^{-10}. Different coolants (deionized water and liquid metal) are adopted and analyzed.

III. RESULTS AND DISCUSSION

We used Eutectic alloy of Ga, In, and Sn, GaInSn (LMTG10B, alloykingdom) as coolant and conducted cooling tests. The inlet temperature is the room temperature 23°C. The chip footprint is 10 mm × 10 mm.

Fig. 3 shows the cooling test results of RTD readings and heater powers as time elapsed. The coolant flowrate is remained constant. The heater power is increased step by step. As the heater power increases, the chip temperatures increase. The chip temperature gradient, indicated by the temperature difference (RTD2 minus RTD1), also enlarges as heater power increases.

The simulation results of GaInSn are compared with the test data as shown in Fig. 4(a). It shows that RTD2 matches with test data, while RTD1 shows a difference. To explore the reason of this discrepancy, we conducted tests using deionized water with the experimental setup in [23-24]. The results show a good agreement in both RTDs in deionized water. That means the simulation models work well. The difference in RTD1 of GaInSn should not be caused by the simulation model.

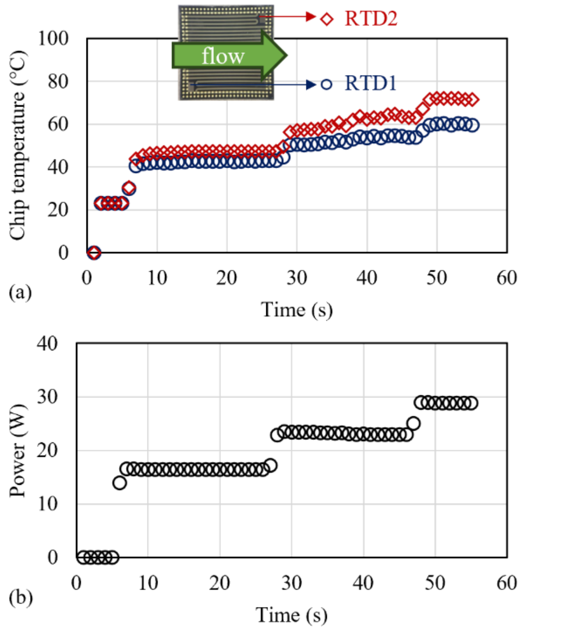

Fig. 3 Cooling test results of GaInSn over time at the inlet velocity of 0.04 m/s. (a) Chip temperatures at RTD1 and RTD2 and (b) chip power.

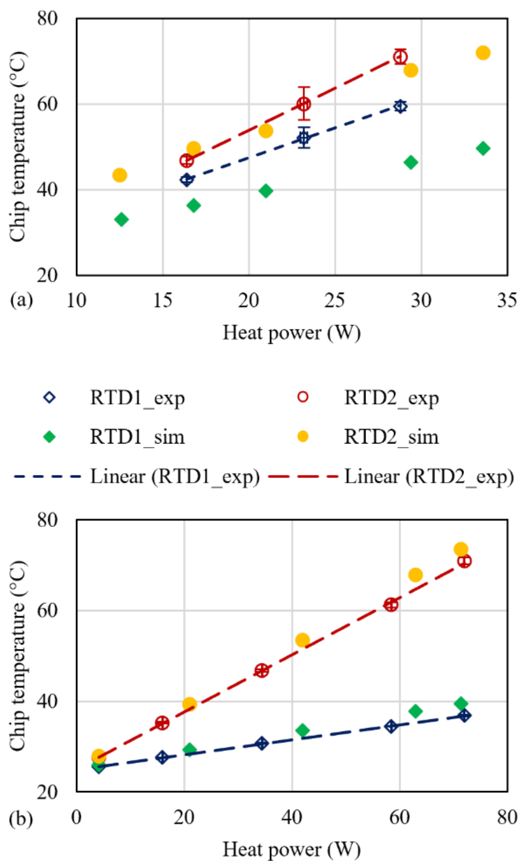

Fig. 4 Simulation model validations. (a) GaInSn and (b) deionized water at the inlet velocity of 0.04 m/s and 0.23 m/s, respectively.

Table I shows that GaInSn has a much larger surface tension compared to other coolants. Surface tension strongly affect flow behavior in microscales. As shown in Fig. 5, coolant enters the chip, expands to chip sides, flows through the micro-pin fins, and exists the chip. In the RTD1 region, in addition to flow along the mainstream direction, the coolant also flows through the micro-pin fins towards the chip sidewall. In the RTD2 region, the coolant already expands well in the chip with micro-pin fins well covered. It generally flows along the mainstream direction and exists at the outlet.

As coolant flows through micro-pin fins, it has to overcome a barrier pressure termed as the Laplace pressure, due to the surface tension. Given by the Young-Laplace equation,

$$\Delta P = -\gamma\left(\frac{1}{R_1}+\frac{1}{R_2}\right) \qquad (1)$$

where γ is the surface tension of coolant, R_1 and R_2 are the principal radii of curvature of the liquid surface. Clearly, the Laplace pressure is proportional to the surface tension, and inversely proportional to the principal radii of curvature.

Liquid coolant passing through the micro-pin fins in this study can be considered as liquid entering the gap between micro-pin fins for simplicity (Fig. 6). The cross section is a ($p \times h$) rectangle, where p and h are pitch and height of micro-pin fins, respectively. From Fig. 6(a), we know $p = 2R_1\cos\theta$, $h = 2R_2\cos\theta$, thus, (1) changes to,

$$\Delta P = -2\gamma\cos\theta\left(\frac{1}{p}+\frac{1}{h}\right) \qquad (2)$$

where θ is the contact angle.

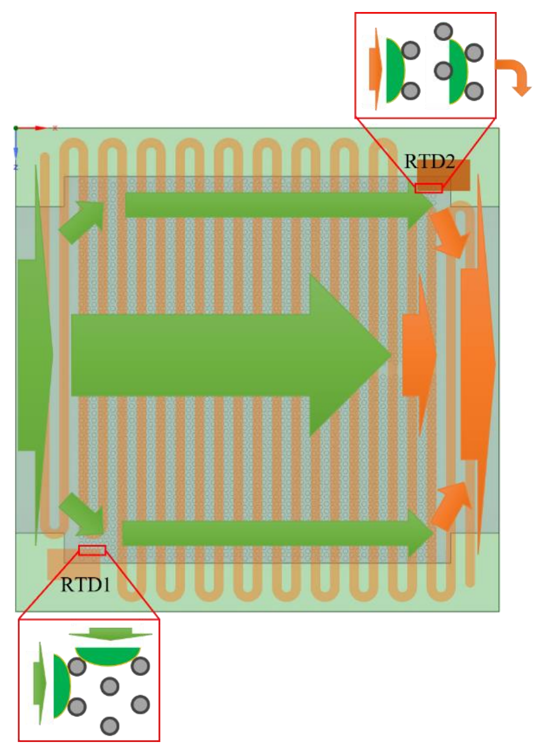

Fig. 5 Schematic illustration of coolant flow expanding at inlet and existing at outlet.

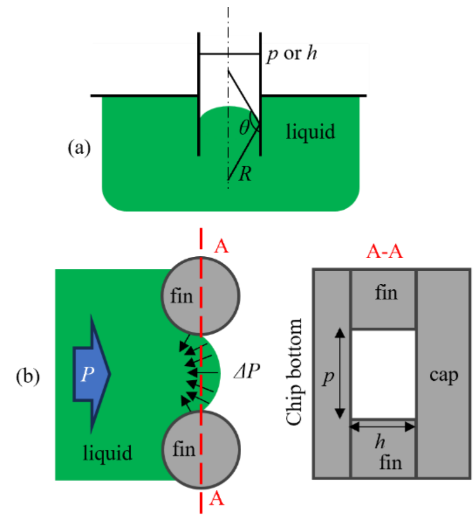

Fig. 6 Schematic illustrations of (a) the surface tension effect and (b) the Laplace pressure ΔP due to the surface tension as coolant passes through micro-pin fins.

From (2), we can see that the Laplace pressure is determined by the coolant surface tension (γ), the fin geometry (p and h), and the contact angle (affected by coolant and chip properties). The surface tension of GaInSn is almost 9 times of that of water. Besides, the contact angle of Ga-based liquid metal on silicon is above 140°, while that of deionized water is 7° [26]. Based on these contact angles and the surface tensions in Table I, we found that the Laplace pressures of GaInSn and deionized water are 10.4 kPa and -1.6 kPa, respectively. The Laplace pressure of deionized water is negative due to its small contact angle, i.e., the good wettability on silicon surface. This good wettability promotes water flow in the micro-cooler. It is evidenced by the good agreement between the simulation and testing results of RTD1 in deionized water cooling.

However, the Laplace pressure of GaInSn acts as a flow resistance, and its value is not insignificant in micro-fluid flow. The coolant flow is driven by the pump along the mainstream direction, thus, the Laplace pressure along this direction can be overcome. However, when coolant expands and reaches RTD1 area, it needs to overcome the Laplace pressure towards the sidewall (Fig. 5). As coolant driving pressure is mainly along the channel, the pressure towards the sidewalls is not large. Hence, coolant has difficulty to reach RTD1 area, which correspondingly leads to a poor cooling and high temperature of RTD1. ANSYS Fluent simulation does not consider the surface tension effect. That means simulation considers full wetting for both water and GaInSn. This is the reason for the well match of water, but poor match of GaInSn at RTD1.

Hence, although GaInSn has a high thermal conductivity, the high surface tension may compromise its cooling performance if the micro-cooler is not properly designed by taking the surface tension effect into consideration. The Laplace pressure can be reduced by increasing the height and/or pitch of micro-pin fins. We remove the micro-pin fins, i.e., making the pitch very large., to minimize the Laplace pressure of GaInSn. The Laplace pressure of GaInSn reduces by 60%, to 4.3 kPa. It will easier for a good wetting of GaInSn. If lyophilic substrates or coatings are used for micro-cooler fabrication, the Laplace pressure can be further reduced [27].

We conducted a numerical simulation and found that GaInSn provides a much lower chip temperature compared to deionized water under the same conditions (Fig. 7). The difference in cooling effectiveness between TTVs with and without pin fins is much smaller when using GaInSn as a coolant compared to deionized water. Therefore, embedded micro-cooler can be greatly simplified by using GaInSn as coolant. Furthermore, the pressure drop of a TTV without pin fins is significantly lower compared to that of a TTV with pin fins. Hence, the pumping power is greatly reduced.

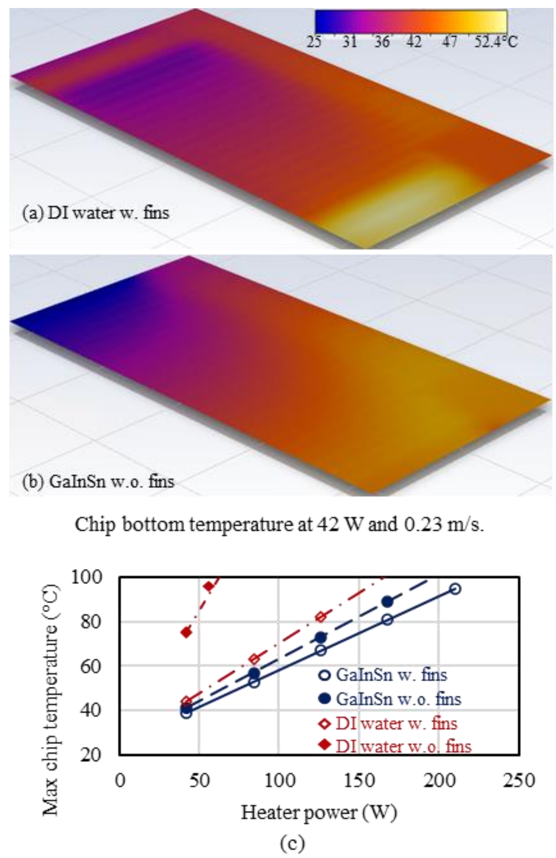

Fig. 7 Temperature distributions of TTV bottom surface using (a) deionized water with fins and (b) GaInSn without fins at heater power of 42 W and coolant inlet velocity of 0.23 m/s; (c) max chip temperature vs. heat power under different conditions at coolant inlet velocity of 0.46 m/s.

Fig. 8 and Fig. 9 shows the cooling performance of GaInSn and deionized water, respectively, without micro-pin fins. We can see that the chip temperature is up to 20°C lower in GaInSn cooling. The pressure drop is higher in GaInSn cooling. But it is not significant in micro-fluid flows. The heat transfer coefficient is around 1.4×10^5 W/m^2.K, 4.2 times of that in deionized water cooling. The coefficient of performance (COP) is slightly lower compared to deionized water.

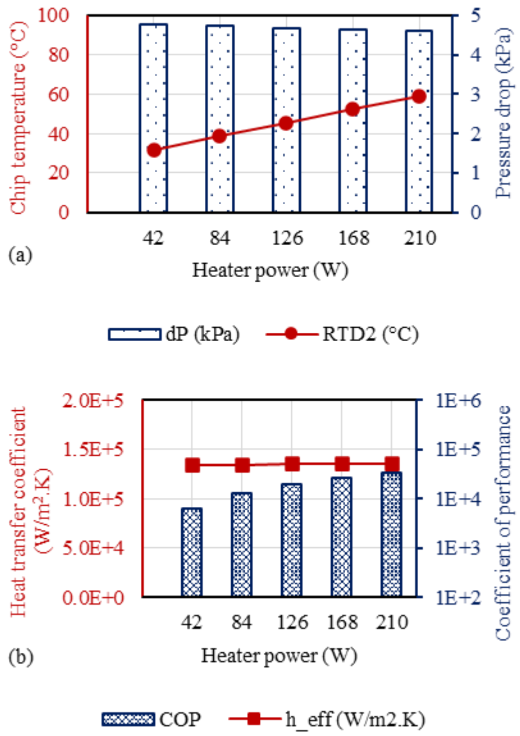

Fig. 8 Cooling performance of GaInSn without micro-pin fins. (a) Chip temperature RTD2 and pressure drop, and (b) heat transfer coefficient h_{eff} and coefficient of performance COP vs. heater power. The coolant inlet velocity is 0.93 m/s.

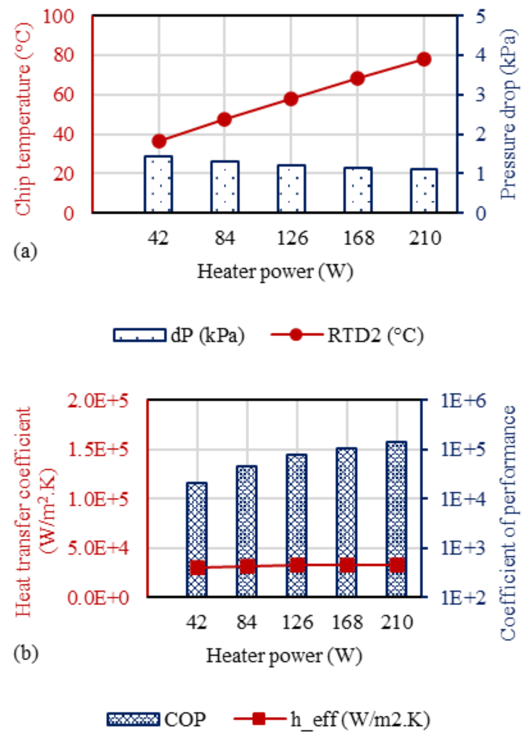

Fig. 9 Cooling performance deionized water without micro-pin fins. (a) Chip temperature RTD2 and pressure, and (b) heat transfer coefficient h_{eff} and coefficient of performance COP vs. heater power. The coolant inlet velocity is 0.93 m/s.

IV. Conclusion

This paper studies embedded liquid metal (GaInSn) cooling of high-power microelectronics by experimental tests and numerical simulations. The experimental tests revealed that a part of the micro-cooler embedded micro-pin fins was not well wetted by GaInSn due to its high surface tension. The analysis on the surface tension effect suggests that the micro-cooler of GaInSn cooling needs customized designs. It would be different from the micro-coolers of conventional coolants (i.e., deionized water, Novec 7300, etc.) as they have much lower surface tensions. To reduces the Laplace pressure (pressure barrier) caused by the high surface tension and large contact angle, we remove the micro-pin fins and found the Laplace pressure is decreased by 60%. The Laplace pressure can be further reduced by using lyophilic substrates or coatings in the micro-cooler.

The numerical simulations showed that GaInSn without micro-pin fins achieved a much lower chip temperature compared to deionized water with micro-in fins thanks to its high thermal conductivity. We also compared the cooling performance of the on micro-coolers without micro-pin fins using GaInSn and deionized water as coolants. The results showed that GaInSn a much lower chip temperature, up to 20°C smaller than that of deionized water. The heat transfer coefficient is 4.2 times to that of deionized water. The pressure drop is larger; however, the coefficient of performance is only slightly lower. This suggests an overall better performance of GaInSn.

This study revealed that the high thermal conductivity of GaInSn greatly advances its cooling performance, however, its high surface tension may be a compromising factor if the micro-cooler is not customized well. Future experimental studies are to be conducted to compare and verify the analysis and simulation, and further facilitate our studies for embedded liquid cooling of 3D ICs (stacked multi-layer functional chips).

References

[1] R.R. Tummala, "Moore's law for packaging to replace Moore's law for ICs," 2019 IEEE Pan Pacific Microelectronics Symposium (Pan Pacific), Kauai, HI, USA, 2019, pp. 1-6.

[2] J.H. Lau, "Recent advances and trends in advanced packaging," IEEE Trans. Compon. Packaging Manuf. Technol., vol. 12, no. 2 (2022), pp. 228-252.

[3] J.H. Lau, "Recent advances and trends in multiple system and heterogeneous integration with TSV-less interposers," IEEE Trans. Compon. Packaging Manuf. Technol., vol. 13, no. 1 (2023), pp. 3-25.

[4] B.P. Behnam, A.K. Sadaghiani, V. Yağcı, Mu. Parlak, K. Sefiane, A. Koşar, "Review on high heat flux flow boiling of refrigerants and water for electronics cooling," Int. J. Heat Mass Trans., vol. 180 (2021), 121787.

[5] A. Bar-Cohen, M. Asheghi, T.J. Chainer, S.V. Garimella, K. Goodson, C. Gorle, R. Mandel, J.J. Maurer, M. Ohadi, J.W. Palko, P.R. Parida, Y. Peles, J.L. Plawsky, M.D. Schultz, J.A. Weibel, Y. Joshi, "The ICECool fundamentals effort on evaporative cooling of microelectronics," IEEE Trans. Compon. Packaging Manuf. Technol., vol. 11, no. 10 (2021), pp. 1546-1564.

[6] S.N. Joshi, F. Zhou, Y. Liu, D.J. Lohan, H. Ukegawa, J. Lee, E.M. Dede. "A review of select patented technologies for cooling of high heat flux power semiconductor devices," IEEE Trans. Power Electron., vol. 38, no. 6 (2023), pp. 6790-6794.

[7] H. Feng, G. Tang, X. Zhang, B.L. Lau, M.C. Jong, K.J. Chui, J. Lou, H. Li, D.V. Le, “Design and development of manifolds for parallel flow and counter flow in two-phase cooling of 3D ICs,” 2022 IEEE 24th Electronics Packaging Technology Conference (EPTC), Singapore, 2022, pp. 880-884.

[8] H. Li, L. Pan, J. Lou, X. Zhang, D.V. Le, M. Cheng, J. Li, C.W. Kang, K.J. Chui, H. Feng, “Numerical simulation for flow boiling in microchannels with different pin fin arrays,” 2022 IEEE 24th Electronics Packaging Technology Conference (EPTC), Singapore, 2022, pp. 1-5.

[9] H. Feng, G. Tang, X. Zhang, B.L. Lau, M.C. Jong, K.Y.J. Au, J.W.J. Ong, K.J. Chui, J. Li, H. Li, D.V. Le, J. Lou, “Development of crossflow manifold for two-phase liquid cooling of 3D ICs via 3D printing,” 2023 IEEE 25th Electronics Packaging Technology Conference (EPTC), Singapore, 2023, pp. 73-77.

[10] G. Tang, L.C. Wai, H. Feng, “Development and demonstration of a novel immersion two phase cooling high power SiC power module,” 2023 IEEE 73rd Electronic Components and Technology Conference (ECTC), Orlando, FL, USA, 2023, pp. 1553-1558.

[11] P. Liu, R. Kandasamy, J.Y. Ho, H. Feng, T.N. Wong, “Comparative study on the enhancement of spray cooling heat transfer using conventional and bio-surfactants,” Appl. Therm. Eng., vol. 194 (2021), 117047.

[12] Y. Zhu, D.S. Antao, D. W. Bian, S.R. Rao, J.D. Sircar, T. Zhang, E.N. Wang, “Suppressing high-frequency temperature oscillations in microchannels with surface structures,” Appl. Phys. Lett., vol. 110, no. 3 (2017), 033501.

[13] J. Mathew, P.-S. Lee, T. Wu, C.R. Yap, “Experimental study of flow boiling in a hybrid microchannel-microgap heat sink,” Int. J. Heat Mass Trans., vol. 135 (2019), pp. 1167-1191.

[14] G. Liang, I. Mudawar, “Review of channel flow boiling enhancement by surface modification, and instability suppression schemes,” Int. J. Heat Mass Trans., vol. 146 (2020), 118864.

[15] D. Deng, L. Zeng, W. Sun, “A review on flow boiling enhancement and fabrication of enhanced microchannels of microchannel heat sinks,” Int. J. Heat Mass Trans., vol. 175 (2021), 121332.

[16] N. Lorenzin, A. Abanades, “A review on the application of liquid metals as heat transfer fluid in concentrated solar power technologies,” Int. J. Hydrog. Energy, vol. 41, no. 17 (2016), pp. 6990-6995.

[17] M. Bilal, K. Ahmad, M.T. Saleem, S. Gulfam, Z. Ahmad, “Recent progress, liquid metal use as plasma facing component and vapor shielding of high heat flux,” Rev. Mod. Plasma Phys., vol. 6 (2022), 9.

[18] Y. Deng, Y. Jiang, J. Liu, “Low-melting-point liquid metal convective heat transfer: a review,” Appl. Therm. Eng., vol. 193 (2021), 117021.

[19] Y. Peng, Y. Xin, J. Zhang, M.D. Dickey, Q. Li, “Functional heterophasic liquid metals,” Responsive Materials, vol. 1, no. 1 (2023), e20230003.

[20] S. Wang, X. Zhao, J. Luo, L. Zhuang, D. Zou, “Liquid metal (LM) and its composites in thermal management,” Compos. Part A Appl. Sci. Manuf., vol. 163 (2022), 107216.

[21] Z. Lin, H. Liu, Q. Li, H. Liu, S. Chu, Y. Yang, “High thermal conductivity liquid metal pad for heat dissipation in electronic devices,” Appl. Phys. A, vol. 124 (2018), 368.

[22] Y. Yerasimou, V. Pickert, S. Dai, Z. Wang, “Thermal management system for press-pack IGBT based on liquid metal coolant,” IEEE Trans. Compon. Packaging Manuf. Technol., vol. 10, no. 11 (2020), pp. 1849-1860.

[23] H. Feng, G. Tang, X. Zhang, B.L. Lau, M.C. Jong, K.Y.J. Au, K.J. Chui, J. Lou, H. Li, D.V. Le, “Embedded micro-pin fin heat sink of two-phase liquid cooling for high heat flux 3D ICs,” 2023 IEEE 73rd Electronic Components and Technology Conference (ECTC), Orlando, FL, USA, 2023, pp. 1964-1968.

[24] H. Feng, G. Tang, X. Zhang, B.L. Lau, M.C. Jong, K.Y.J. Au, J.W.J. Ong, K.J. Chui, J. Li, H. Li, D.V. Le, J. Lou, “Two-phase liquid cooling for high-power microelectronics via embedded micro-pin fin heat sink”, unpublished.

[25] B.L. Lau, J. Ong, J. Au, M.C. Jong, X. Zhang, H. Feng, “Wafer level fabrication of embedded silicon microchannel on heating devices,” 2023 IEEE 25th Electronics Packaging Technology Conference (EPTC), Singapore, 2023, pp. 686-689.

[26] I.D. Joshipura, K.A. Persson, V.K. Truong, J.-H. Oh, M. Kong, M.H. Vong, C. Ni, M. Alsafatwi, D.P. Parekh, H. Zhao, M.D. Dickey, “Are contact angle measurements useful for oxide-coated liquid metals?” Langmuir 37, no. 37 (2021), pp. 10914-10923.

[27] Z.-Y. Zhao, T. Li, Y.-R. Duan, Z.-C. Wang, H. Li, “Wetting and coalescence of the liquid metal on the metal substrate,” Chin. Phys. B, vol. 26, no. 8 (2017), 083104.